Bioconjugate Chemistry

Article

pubs.acs.org/bc

Cell Uptake and Localization Studies of Squaramide Based Fluorescent Probes

Angel Sampedro,[†] Ruth Villalonga-Planells,[†] Manuel Vega,[†] Guillem Ramis,[‡] Silvia Fernández de Mattos,[‡] Priam Villalonga,[‡] Antoni Costa,*[,†] and Carmen Rotger*[,†]

[†]Departament de Química, [‡]Departament de Biologia Fonamental, Institut Universitari d'Investigació en Ciències de la Salut (IUNICS) and Instituto de Investigación Sanitaria de Palma (IdISPa), Illes Balears, Spain, Universitat de les Illes Balears, Ctra. Valldemossa km 7.5, 07122 Palma, Spain

Supporting Information

ABSTRACT: Cell internalization is a major issue in drug design. Although squaramide-based compounds are receiving much attention because of their interesting bioactivity, cell uptake and trafficking within cells of this type of compounds are still unknown. In order to monitor the cell internalization process of cyclosquaramide compounds we have prepared two fluorescent probes by covalently linking a fluorescent dye (BODIPY derivative or fluorescein) to a noncytotoxic cyclosquaramide framework. These two probes (C2-BDP and C2-FITC) rapidly internalize across live cell membranes through endocytic receptor-mediated mechanisms. Due to its higher fluorescence and photochemical stability, C2-BDP is a superior dye than C2-FITC. C2-BDP remains sequestered in late endosomes allowing their fast and selective imaging in various live cell types. Cyclosquaramide−cell membrane interactions facilitate cell uptake and have been investigated by binding studies in solution as well as in live cells. Cyclosquaramide **1** (C2-BDP) can be used as a highly fluorescent probe for the rapid and selective imaging of late endosomes in live cells.

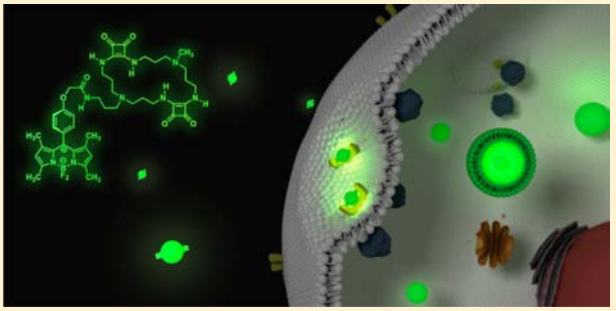

INTRODUCTION

The ability to overcome biological barriers determines the effectiveness of drugs and probes aimed at subcellular targets. Therefore, cell uptake constitutes one major challenge in the design of bioactive molecules. In terms of lipophilicity, only molecules within a narrow range of Log P values may be useful in biological applications. However, with the broad range of bioactive compounds available, cell permeability must be enhanced through diverse transport strategies such as the use of nanocarriers,[1,2] liposome encapsulation,[3] electroporation,[4] or microinjection.[5] As drawbacks, these methodologies present important toxicity levels and cell damage that prevent their extended application in drug delivery. In contrast, some molecules of natural origin can effectively cross the cell membrane through facilitated transport pathways triggered by the formation of hydrogen bond and electrostatic interactions between the compound and a cell membrane receptor or the cell membrane surface. Thus, the hydrogen bonding ability is important for membrane−compound interactions and has a positive effect on uptake in living cells. In fact, the effectiveness of certain natural cell-penetrating peptides (CPPs) has been attributed to the presence of numerous basic amino acids (primarily arginines) in their primary structure. Internalization of CPPs is triggered by binding the arginine guanidinium group to anionic compounds located at the cell membrane surface,[6−8] showing that the combination of hydrogen bonding and electrostatic interactions provides a powerful tool for designing specific recognition systems that could facilitate the cell uptake.

Recently, we investigated the biological activity of a series of cyclic squaramide compounds in cultured cells showing their potential as a new class of anticancer drugs.[9] Due to its unique structural features, the squaramide unit is receiving special attention nowadays. Considered a bioisostere of the guanidinium group, squaramides[10] have been successfully incorporated in compounds with interesting antiparasitic,[11,12] antibiotic,[13] antitumor, and kinase inhibitory activity,[14,15] among others. However, in spite of the increasing number of bioactive squaramide-based compounds found in the literature, their cellular uptake and trafficking within the cell have still not been investigated.

Squaramides are excellent molecular recognition units[16−19] due their capacity to establish cooperative hydrogen bonds.[20−22] The combination of squaramide moieties with tetralkylammonium groups has led to hosts that strongly bind oxoanions, such as phosphate, sulfate, and carboxylate, in water−ethanol mixtures.[23−27] All these features suggested that squaramide-based compounds could internalize into the cell, mimicking the CPP's performance. With the aim to investigate

Received: June 10, 2014
Revised: July 17, 2014
Published: July 18, 2014

   dx.doi.org/10.1021/bc500258b | *Bioconjugate Chem.* 2014, 25, 1537−1546

the cellular uptake and trafficking within the cell of cylosquaramide compounds, we have prepared the cyclosquaramide fluorescent probes **1** and **2** (Figure 1). These two probes combine the cyclosquaramide framework with common fluorescent dyes.

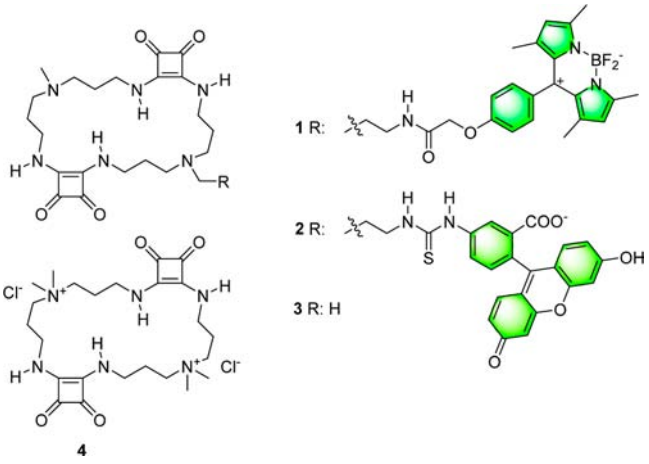

Figure 1. Structure of cyclosquaramide-based fluorescent probes **1**−**2** and cyclosquaramides **3** and **4**.

In this study, we chose the smallest cyclosquaramide of the previously reported series containing only two squaramide units, because of its demonstrated low toxicity levels (IC_{50} > 200 μM) in different cell lines.[6] The dyes are a BODIPY (4,4-difluoro-4-bora-3*a*,4*a*-diaza-*s*-indacene) derivative **8**[28] and fluorescein. At physiological pH, these dyes are zwitterionic and anionic, respectively, and they were chosen in order to demonstrate the potential of this small cyclosquaramide as a low molecular weight cell penetrating compound.

RESULTS AND DISCUSSION

Synthesis of Fluorescent Cyclosquaramides. Briefly, the synthesis of probes **1** and **2** was performed following a modular approach and is outlined in Scheme 1. First of all, we prepared the cyclosquaramide **13** as the macrocyclic scaffold decorated with an amino-protected alkyl chain as a linker. The macrocyclization step was achieved by condensation of the disquaramide diethyl ester **9** with diamine **12**.[29] Cleavage of the Boc-amino-protecting group followed by condensation with acid **8** or fluorescein isothiocyanate (FITC) yielded the fluorescent cyclosquaramide probes **1** (C2-BDP) and **2** (C2-FITC), respectively.

Photochemical Studies. The photophysical parameters of cyclosquaramides **1** and **2** were assessed in aqueous solutions. C2-BDP and C2-FITC show absorption maxima at 500 nm (ε = 46 448 M^{-1} cm^{-1}) and 495 nm (ε = 47 794 M^{-1} cm^{-1}) and fluorescence emission at 510 and 525 nm, respectively (Figure 2a,b). The relative fluorescence intensity was normalized using Oregon Green 488 (OG, φ = 0.97, borate buffer 0.1 M, pH 9) as standard and was measured at pH 5.5 and 7.4. The quantum yields obtained at pH 7.4 were reasonably high [φ = 0.10 (C2-BDP) and φ = 0.22 (C2-FITC)] for fluorescent probes in water. The maximum fluorescence intensity measured was 10−20% of that of OG due to quenching of the fluorophores by PET arising from the donor squaramide rings[30] and lone pairs of the tertiary amino groups.

The pH dependence of fluorescence emission for cyclosquaramides **1** and **2** was also investigated (Figure 2c). C2-BDP showed a 5-fold increase in fluorescent signal emission in acidic conditions (pH < 6), and the quantum yield obtained for C2-BDP at pH 5.5 (φ = 0.15) was slightly higher than that measured at neutral pH. This suggests that, in acidic media, protonation of the tertiary amines (pK_{a1} = 7.9 ± 0.2; pK_{a2} = 8.6 ± 0.1) occurs and prevents the fluorophore quenching due to the nitrogen lone pair. Comparatively, C2-FITC showed maximum fluorescent emission at neutral pH, where the fluorescein moiety is in its dianionic form (pK_{a1} = 4.3 and pK_{a2}

Scheme 1. Synthesis of Cyclosquaramides 1−3[a]

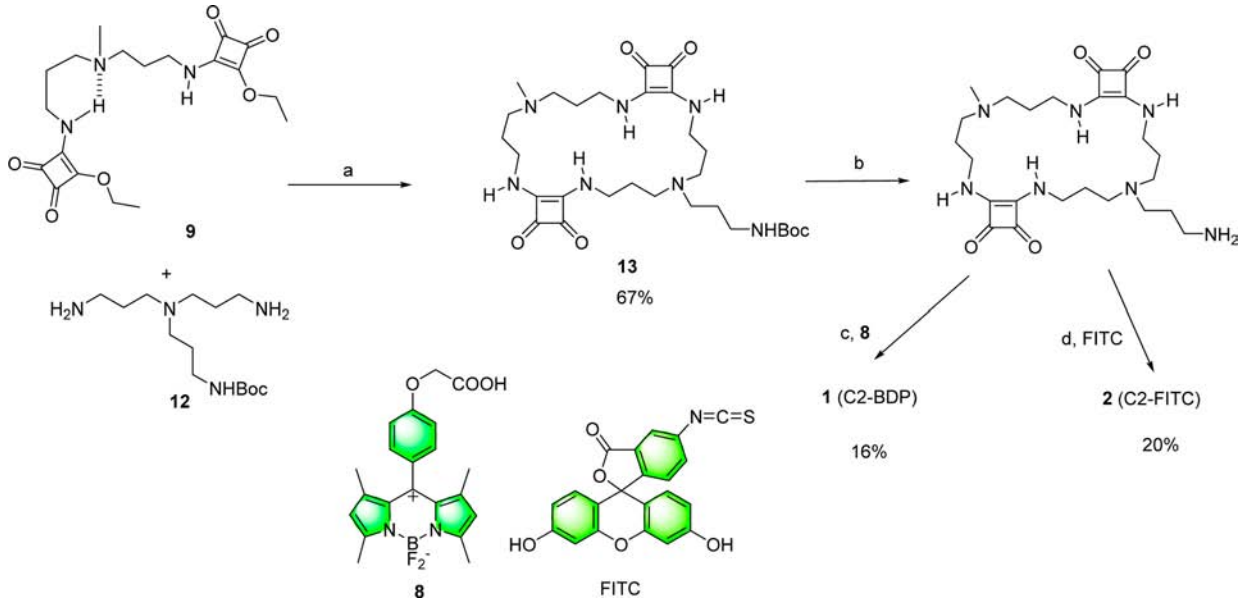

[a]Reagents and conditions: (a) EtOH; (b) HCl−MeOH, (c) **8**, TSTU, DiPEA, NMP, (d) DiPEA, DMSO.

dx.doi.org/10.1021/bc500258b | *Bioconjugate Chem.* 2014, 25, 1537−1546

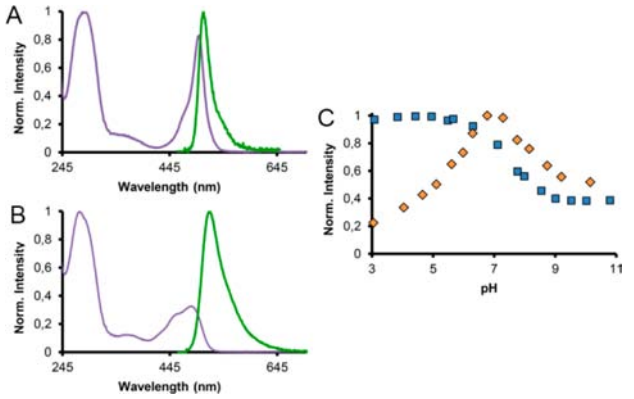

Figure 2. (A,B) Normalized absorption (purple) and emission (green) spectra of 5×10^{-5} M solution of cyclosquaramides **1** and **2** at pH 7.4 in PBS−DMSO 1%. Emission spectra have been recorded at 465 and 470 nm, respectively, to avoid dispersion of the excitation emission band overlapping. (C) Fluorescence vs pH curves of **1** (blue) and **2** (yellow) 5×10^{-6} M solution at pH varying from 3 to 11 in H_2O−DMSO 1% with 0.1 M NaCl of ionic strength.

= 6.8)[31] and the cyclosquaramide tertiary amines are partially protonated. At a basic pH > 8, C2-FITC fluorescence decreases due to the squaramide and tertiary amine quenching effect.

Binding Studies. To measure the intrinsic affinity of the cyclosquaramide-based fluorescent probes for anions, we determined the association constants of the model cyclosquaramide **4** with a selection of anionic phosphate compounds capable of mimicking anionic phosphate membrane components via isothermal titration calorimetry (ITC) in water at 25 °C. The selected phosphates were adenosine monophosphate (AMP), fructose-1,6-biphosphate (FBP), and mannose-6-phosphate (M6P). We used cyclosquaramide **4** for these experiments because the two tetraalkylammonium groups in its structure constitute a good model of a fully protonated cyclosquaramide and, hence, of a positively double-charged structure that has the ability to establish electrostatic interactions through its positively charged centers, while avoiding the interference of the protonation equilibrium at its basic centers in aqueous media. To run these studies, a 3:1 molar mixture of **4** and the corresponding phosphate in water was titrated against an HCl solution (Figure 3).

The obtained binding constants and thermodynamic parameters are shown in Table 1. For further detail on the fitted equilibria, see Supporting Information (SI) Tables S1−S8. The distributions of species along pH are represented in Figures S4−S9 in the SI. At pH 7.4, the phosphate compounds AMP and M6P are dianionic and FBP is tetraanionic. Analysis of the titration data revealed that at physiological pH, **4** forms 1:1 complexes with M6P, AMP, and FBP, and the association constants obtained for, **4·M6P**, **4·AMP**, and **4·FBP** were K_{as} = 4.4×10^3 M^{-1}, 2.1×10^5 M^{-1}, and 2.5×10^6 M^{-1}, respectively. These values indicate the existence of a strong affinity of the cyclosquaramide moiety for negatively charged phosphate compounds in water.

Cell Uptake and Localization Studies. The cell internalization capability of cyclosquaramide probes **1** and **2** was investigated. Human glioblastoma cells (U87MG) were treated with a 10 μM solution of each fluorescent probe for 1 h at 37 °C. Thereafter, the cellular fluorescence emission was evaluated using flow cytometry and confocal fluorescence microscopy. The two fluorescent probes were readily internalized and

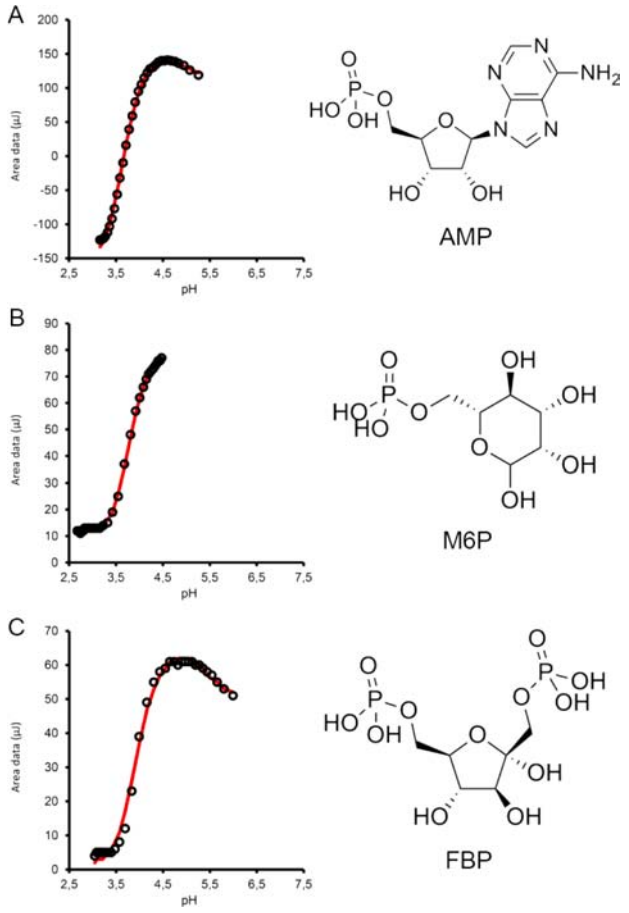

Figure 3. ITC Data: experimental data (○) and curve fitting (red line) for the formation of the complex of cyclosquaramide **4** with (A) adenosine monophosphate, (B) mannose-6-phosphate, and (C) fructose-1,6-biphosphate in H_2O at 25 °C.

Table 1. Summary of the Binding Constants and Thermodynamic Parameters Obtained for Complex Formation of Cyclosquaramide 4 and Phosphate Compounds in H_2O by ITC at 25 °C

complex	log β	K_{as} (M^{-1})	ΔH (kJ mol^{-1})	ΔS (J mol^{-1})
4·M6P	3.64	4.4×10^3	17.0 ± 6	127
4·AMP	5.32	2.1×10^5	16.4 ± 0.6	157
4·FBP	6.4	2.5×10^6	−10.1 ± 0.8	89

accumulated in vesicle-like structures in the cytosol (Figure 4). Furthermore, when U87MG cells were treated with the fluorophores alone (i.e., ethyl ester of **8** and FITC) under the same experimental conditions, intracellular fluorescence was not detected, which emphasizes the role of the cyclosquaramide moiety in the internalization of the fluorescent probes (see SI Figure S14).

Interestingly, the staining patterns of C2-BDP and C2-FITC revealed well-defined punctated subcellular structures located at the perinuclear region of the cells, but the confocal images indicated that the fluorescent regions in the C2-FITC stained cells were not as bright as those treated with C2-BDP. This suggests that the probes are confined in an acidic environment, lowering the C2-FITC fluorescence and enhancing the emission of C2-BDP.

Taking advantage of the activation of the C2-BDP probe within the cell, we selected this compound to complete our

dx.doi.org/10.1021/bc500258b | Bioconjugate Chem. 2014, 25, 1537−1546

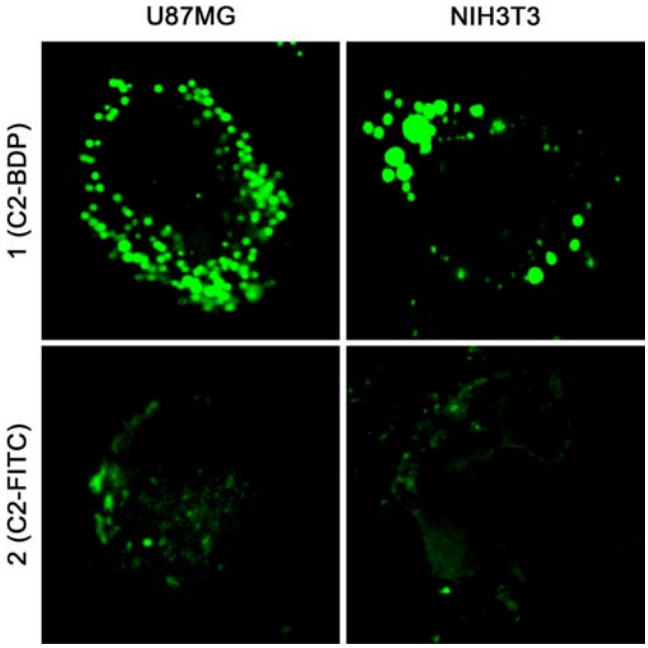

Figure 4. Confocal images of U87MG and NIH3T3 cells stained with cyclosquaramides **1** (top) and **2** (bottom): The cells were incubated with the compounds at a concentration of 10 μM for 1 h at 37 °C.

studies. Furthermore, BODIPY-derived probes are widely used in biological applications due to their superior photochemical properties, such as high quantum fluorescence yields, high molar extinction coefficients, narrow absorption and emission spectra, and high photochemical stability.[32−34] Consequently, C2-BDP fluorescent emission was stable after more than 70 excitation−emission cycles in PBS solution, and once internalized in live cells remained sequestered in vesicle-like compartments up to 24 h after cell treatment. The fluorescence emission remained also stable for longer than 50 h in live cells (see SI Figures S3 and S13).

To optimize C2-BDP working conditions in live cells, dose−response and time-course experiments were conducted in NIH3T3 (nontransformed mouse fibroblast cells) and U87MG cells. Optimal images showing a highly punctated perinuclear distribution of C2-BDP were obtained when cells were incubated with a 10 μM solution the probe for 1 h. Cell penetration of C2-BDP was detected after only 5 min incubation, which indicated that cellular internalization is an effective and rapid process (see SI Figures S12 and S13).

The cytotoxic effect of compound C2-BDP (10 μM) on NIH3T3, Jurkat (human T lymphocyte cells), and U87MG cells was negligible, as cell viability in all cell lines was higher than 90% after 48 h of treatment (see SI Figure S10).

Confocal fluorescence microscopy was performed to assess the intracellular localization of C2-BDP in live cells (Figure 5 and SI Figure S17). U87MG and NIH3T3 cells were stained with C2-BDP and organelle-specific red fluorescent probes (BacMam System, Life Technologies, Carisbad, California, U.S.) used for comparison. BacMam-RFP probes use baculovirus as the vehicle for the delivery and expression of genes, and we did not expect any mutual exclusion effect with C2-BDP. Quantitative colocalization analysis was made determining Pearson's correlation coefficient (P) and the Mander's overlap coefficients ($M1$ and $M2$).[35] As shown in Figure 5, C2-BDP did not colocalize with either lysosome (P = 0.26, $M1$ = 0.36, $M2$ = 0.40) or Golgi apparatus-specific probes (P = 0.42, $M1$ = 0.27, $M2$ = 1). However, the distribution of C2-BDP partially overlapped with early endosomes (P = 0.52, $M1$ = 0.82, $M2$ = 0.90) and completely colocalized with late endosomes (P = 0.91, $M1$ = 0.95, $M2$ = 0.97) indicating that C2-BDP accumulates within these acidic organelles.

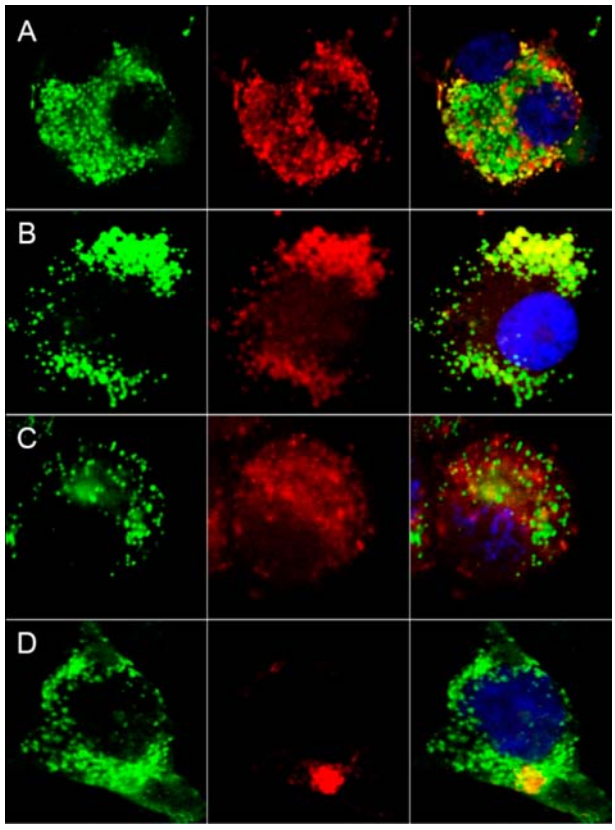

Figure 5. Confocal imaging of U87MG cells containing 10 μM C2-BDP for 1 h and BacMam-RFP specific probes for (A) early endosomes, (B) late endosomes, (C) lysosomes, and (D) the Golgi apparatus. Left column: C2-BDP (green), middle column: RFP probes (red), and right column: overlay (orange) with DAPI staining of cell nuclei (blue).

These results are consistent with the weak basic nature of the cyclosquaramide and the fluorescence activation observed before. In energy-dependent endocytic pathways, late endosomes originate when uncoated vesicles ultimately fuse with early endosomes (pH 6.3), which then mature and become more acidic (pH 5.5). In this process, the size and morphology of the endosomes change, and they move toward the perinuclear region of the cell. Eventually, late endosomes fuse with lysosomes, generating even more acidic organelles (pH 4.7).[36] Therefore, many weak basic polyamines can be localized to acidic vesicles such as endosomes or lysosomes.[37−40] However, our probe remained within the late endosomal lumen and avoided lysosomes, suggesting that it shows distinct trafficking activity compared to LysoTracker, which is a specific lysosome marker with structural features akin to C2-BDP. Furthermore, other commercially available fluorescent markers such as ER-Tracker and BODIPY FL that contain BODIPY dyes linked to small organic molecules selectively stain the endoplasmic reticulum and Golgi apparatus, respectively.

The results obtained from the initial cell uptake and localization studies evidence that the cyclosquaramide moiety and, hence, its capability to establish specific supramolecular

dx.doi.org/10.1021/bc500258b | *Bioconjugate Chem.* 2014, 25, 1537−1546

interactions with some cell components determines not only the permeability of this probes, but also its final localization within the cell. In this sense, the C2-BDP probe can be used to rapidly and selectively stain late endosomes in live cells. This is a novelty since to our knowledge the commercially available late endosome fluorescent markers are based on the use of fluorescent proteins. The application of these systems implies the combination of two different processes: signal transduction and selective labeling. The assays based on this methodology are usually time-consuming, and overexpressed proteins are often ubiquitously localized and, therefore, not specific in their localization.

Additionally, the endosomal localization of the cyclosquaramide compound prevents the action of lysosomally activated hydrolases on the compound and can be attributed either to a specific internalization pathway or to deprivation of the signals required for fusion with other cellular compartments along the endocytic pathway.

To gain further insight into the cellular internalization and the trafficking properties of C2-BDP, we performed additional experiments. We first conducted a parallel artificial permeability assay (PAMPA) to evaluate C2-BDP permeability in vitro.[41,42] The observed absence of passive transport strongly suggested that the internalization of C2-BDP through the cell membrane is related to an energy-dependent active transport pathway. To confirm this observation, cultured cell lines (NIH3T3 and U87MG) were treated with C2-BDP (10 μM) for 30 min at 4 °C, and uptake was evaluated via flow cytometry. At this temperature, energy-dependent internalization processes are prevented. Under these conditions, C2-BDP uptake was significantly reduced in both cell types compared to the uptake observed at 37 °C (Figure 6 and SI Figure S15). Therefore, C2-BDP internalization is a concentration-, time-, and energy-dependent process, which may be related to a specific mechanism of uptake.

Several common energy-dependent endocytic pathways involve receptor-mediated mechanisms, including clathrin- and caveolin-mediated endocytosis.[43,44] To explore the existence of a recognition event at the cell membrane, we performed competition experiments by preincubating cells with various compounds that are capable of inhibiting a membrane receptor response, before treating the cells with C2-BDP. First, we used cyclosquaramide **3** as a competitive agent, which is a nonfluorescent compound that retains the same macrocyclic framework as C2-BDP and could therefore establish the same supramolecular interactions due to the cyclosquaramide moiety and the two basic centers with a membrane receptor. NIH3T3 and U87MG cells were thus pretreated with **3** (50 μM, 1 h at 37 °C), followed by treatment with C2-BDP (10 μM, 1 h at 37 °C). As expected, internalization was reduced to only 30% of that observed in control conditions (Figure 6).

Furthermore, C2-BDP internalization was also inhibited when cultured cells were pretreated with chlorpromazine and nystatin, which are specific inhibitors of clathrin and caveolin-mediated endocytosis, respectively.[43] As shown in Figure 7a, the inhibition of the uptake mechanism is cell type dependent. When cells were treated with dynasore, an inhibitor of the GTPase dynamin, which is involved in both pathways and is responsible for endocytic vesicle formation, 80% inhibition of the uptake of C2-BDP was observed. Taken together, these results confirm that a receptor-mediated endocytotic process is an integral part of the C2-BDP uptake mechanism.

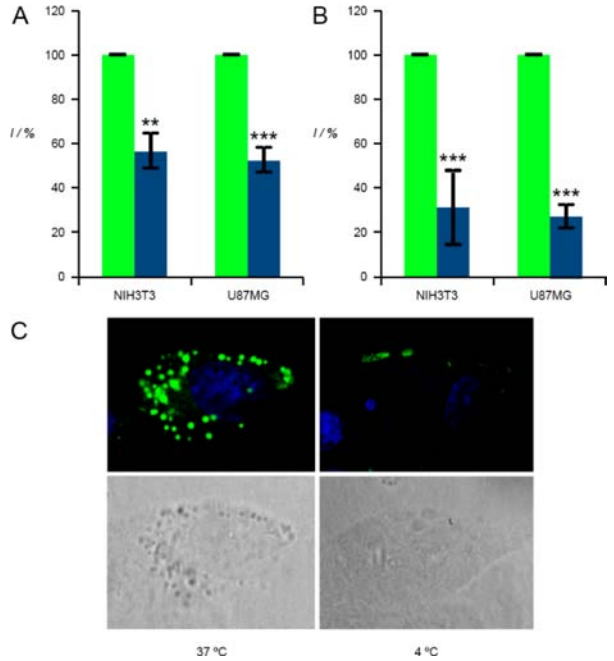

Figure 6. Inhibition of C2-BDP uptake: (A) incubation of NIH3T3 and U87MG cells with C2-BDP (10 μM, 1 h) at 37 °C (green) and 4 °C (blue); (B) incubation of NIH3T3 and U87MG cells with cyclosquaramide **3** (50 μM, 1 h) at 37 °C, followed by C2-BDP treatment (10 μM, 1 h) at 37 °C (blue). Control cells were treated with C2-BDP alone (10 μM, 1 h) at 37 °C (green). The data are presented as the mean ± SD of the fluorescence intensity from three independent experiments performed in duplicate and are expressed as the percentage of the intensity relative to the control (green). The differences between C2-BDP alone and the cotreatments were statistically significant (Student's t test: $^{**}P < 0.01$ and $^{***}P < 0.001$, respectively). (C) Confocal images of U87MG cells treated with C2-BDP (10 μM) at 37 °C and 4 °C.

The initial binding of cyclosquaramides at the outer cell membrane that precedes endocytosis can be explained by the high affinity of squaramides for oxoanionic groups present on the external side of the membrane (Figure 7b). Membrane proteins such as heparin sulfate proteoglycans or minor membrane components such as phosphatidic acids can interact with the slightly basic cyclosquaramides. High affinity was observed in live cells. U87MG cells were treated with C2-BDP (10 μM) at 4 °C for 30 min and subsequently washed. The resultant confocal images showed that the fluorescent compound remained bound to some domains on the cell membrane surface, suggesting interaction specificity (Figure 6b and SI Figure S16).

To determine the significance of this interaction in live cells, the same experiment was performed, treating a fixed number of 10^4 cells with increasing concentrations (0–60 μM) of C2-BDP at 4 °C to prevent endocytosis. The cells were washed to eliminate weakly adsorbed molecules, and the remaining fluorescent compound bound to the cell membrane was quantified by measuring the fluorescent signal intensity in the cell lysate solution. Global analysis of single-site and nonspecific binding revealed a K_d = 5.9 μM and a maximum specific binding, B_{max} = 201 a.u. (SI Figure S18). These values indicated that the total approximate amount of bound C2-BDP was 13.2 pg/cell.[45] The association constant obtained in vivo was of the same order of magnitude as that obtained for compound **5** and the model phosphate compounds in solution and is also in

dx.doi.org/10.1021/bc500258b | Bioconjugate Chem. 2014, 25, 1537–1546

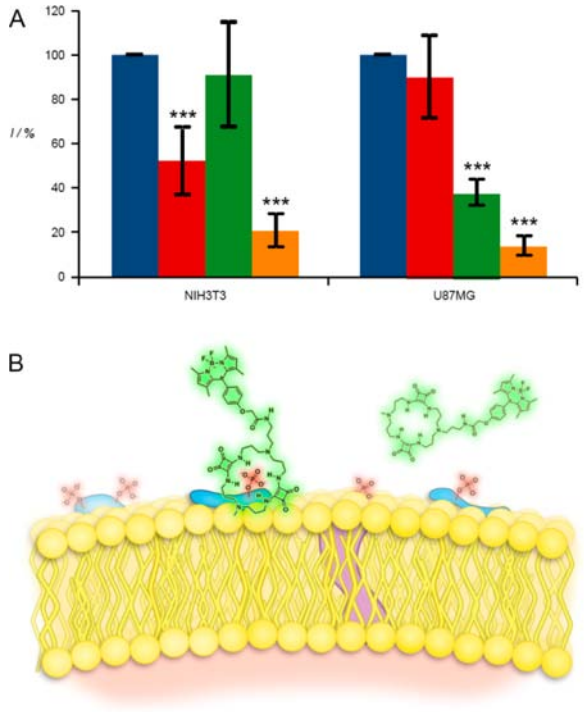

Figure 7. (A) Uptake inhibition of C2-BDP in NIH3T3 and U87MG cells treated with chlorpromazine (red), nystatin (green), or dynasore (orange), followed by treatment with 10 μM C2-BDP, as compared to control cells treated with C2-BDP alone (blue). The data are presented as the mean ± SD of the fluorescence intensity from three independent experiments performed in duplicate and are expressed as the percentage of the intensity relative to the control (blue). The differences between C2-BDP alone and the cotreatments were statistically significant (Student's *t* test: ***$P < 0.001$). (B) Schematic representation of the adsorption of C2-BDP at the cell membrane.

agreement with reported values for small molecule−macromolecule interactions on cell membranes.[46]

Mannose-6-phosphate (M6P) plays an important role in subcellular trafficking.[47] Mammalian cells possess two M6P receptors, CD-MPR and CI-MPR, which are transmembrane proteins that bind M6P-tagged hydrolytic enzymes in the Golgi and mediate their trafficking to late endosomes. Upon arrival at the endosomes, the low pH causes the release of the hydrolases from the receptor and their subsequent activation when late endosomes fuse with lysosomes. In correlation with its ability to interact with phosphate compounds, the binding studies show that cyclosquaramide **4** can bind to the M6P moiety, with a dissociation constant for the **4·M6P** complex at pH 5.5 of K_d = 23 × 10^{-5} M, which is 1 order of magnitude lower than the value obtained using a recombinant single-chain antibody fragment against M6P.[48]

This result suggests that in late endosomes, C2-BDP could interact with mannose-6-phosphate residues and alter the activation of hydrolases, which might disturb late endosome maturation. This may explain the prolonged localization of C2-BDP in this subcellular compartment.

CONCLUSION

We have synthesized two fluorescent cyclosquaramides probes that rapidly internalize across live cell membranes. Cell uptake and localization studies indicate that C2-BDP probe internalizes into the cell through endocytotic receptor-mediated mechanisms and remains sequestered in late endosomes. This behavior can be attributed to the role of the cyclosquaramide framework and its supramolecular interaction capabilities. Thus, the strong affinity of cyclosquaramides for anionic phosphate compounds present on the cell membrane triggers the internalization process and explains the specific localization observed inside the cell. Accordingly, cyclosquaramide **1** (C2-BDP) can be used as a highly fluorescent probe for the rapid and selective imaging of late endosomes in live cells.

EXPERIMENTAL PROCEDURES

General Information. All chemicals of the highest quality were purchased from Aldrich, and were used without further purification unless otherwise stated. CellLight BacMan 2.0 system reagents were purchased from Invitrogen Life technology, CellTiter-Glo Luminescent Cell Viability Assay was purchased from Promega. [D6] DMSO and $CDCl_3$ (99.8% D) were stored on molecular sieves (3 Å). Routine NMR spectra were recorded using a Bruker Avance 300 MHz. Chemical shifts of ^{1}H and ^{13}C NMR signals were quoted to the residual peaks $CDCl_3$ or [D_6]DMSO, respectively, and expressed by chemical shifts in ppm (δ), multiplicity, coupling constant (Hz), and relative intensity. RP-HPLC was used as the purification technique for final products **1**−**3** in a GILSON system equipped with 321 pump and UV−vis-152 detector modules. UV−vis measurements were obtained on a (UV−vis) Varian Cary 300 Bio spectrophotometer. Fluorescence measurements were obtained on a Varian Cary Eclipse spectrophotometer. Isothermal titration calorimetry experiments were run on a NanoITC III from TA Instruments. MS spectra were recorded on a Micromass Autospec 3000 (HRMS−ESI) and Bruker Autoflex (MALDI−TOF) with trans-2-[3(4-*t*-butylphenyl)-2-methyl-2 propenylidene]-malononitrile (DCTB) as matrix. Luminescence was measured using a Synergy Mx microplate reader, Biotek Instruments Inc. Cell fluorescence was measured on Beckman Coulter Epics XL-MLC flow cytometrer. Fluorescent confocal laser scanning microscopy was performed with a Confocal Scanner TCS SP2 Leica, from Leica Microsystem, Heidelberg.

Synthesis. Acid **8** was synthesized following the synthetic route described elsewhere.[14] For a detailed procedure of the synthesis of **8** and **12**, see Supporting Information.

Synthesis of Cyclosquaramide ***13***. **9** (1.80 g, 4.58 mmol) in EtOH (30 mL) was warmed at 50 °C until complete dissolution. To this solution, **12** (1.32 g, 4.58 mmol) in EtOH (20 mL) was added dropwise. The mixture was stirred overnight under argon atmosphere at room temperature. The precipitate formed was filtered and cleaned with EtOH (4 × 10 mL) and Et_2O (2 × 10 mL), to obtain a pale yellow solid. The crude product was washed in boiling acetone (3 × 20 mL) and dried under vacuum obtaining the final product **13** (1.82 g, 3.09 mmol) as a pale yellow solid. Yield: 67%.

^{1}H NMR (300 MHz, DMSO-d_6, 25 °C): δ = 1.37 (s, 9H; *t*Bu), 1.47 (br, 2H; CH_2CH_2NHBoc), 1.64 (br, 8H; $CH_2CH_2CH_2$), 2.11 (s, 3H; NCH_3), 2.33 (br, 10H; CH_2N), 2.91 (br, 2H; CH_2NHBoc), 3.50 (br, 8H, CH_2NH(Sq)), 6.75 (br, 1H, NHBoc), 7.40 (br, 4H, NH(Sq)); ^{13}C NMR (75 MHz, DMSO-d_6, 25 °C) δ = 26.7, 28.0, 28.2, 37.97, 41.7, 50.4, 54.2, 77.3, 155.6, 167.8, 182.3. HRMS (ESI) calcd for 612.3486 (M +Na; $C_{29}H_{47}N_7O_6Na^+$), found 612.3480.

Synthesis of Cylosquaramide ***1***. **13** (0.32 g, 0.55 mmol) was treated with 8 equiv of aqueous HCl (4.4 mmol, 10 mL) and stirred overnight at 50 °C. Then, the solution was basified with

dx.doi.org/10.1021/bc500258b | *Bioconjugate Chem.* 2014, 25, 1537−1546

a saturated solution of Na_2CO_3 to pH 9 and concentrated under vacuum to obtain the free amine as a yellowish solid, which was used without further purification into the next step. The complete cleavage of the Boc-group was verified by ^{1}H NMR. The free amine of **13** was dissolved in 1-methyl-2-pyrrolidinone NMP (2 mL) with 3.6 equiv of DiPEA (193.3 μL, 1.11 mmol) and filtered to remove inorganic salts. Apart, **8** (121 mg, 0.3 mmol) and DiPEA (71.4 μL, 0.41 mmol) were dissolved in NMP (4 mL). To this solution, *N,N,N′,N′*-tetramethyl-*O*-(*N*-succinimidyl)uranium tetrafluoroborate, TSTU (92 mg, 0.3 mmol) in NMP (2 mL) were added and the mixture was stirred for 90 min protected from light at room temperature and under argon atmosphere. After this, both solutions were mixed and stirred overnight at room temperature, protected from light and under argon atmosphere. Then, the orange solution was filtered and cold Et_2O (15 mL) was added to the crude solution to separate a dark oil which was decanted and cleaned successively with Et_2O (15 mL) and pentane (10 mL) yielding an orange solid. The crude was purified by RP-HPLC (Column: Atlantis Prep T3 OBD 5 μm, 19 × 150 mm, from Waters. Mobile phase: Eluent A (H_2O, 10 mM $AcONH_4$, pH 4.5); Eluent B (acetonitrile)) to obtain **1** as a dark orange solid (42 mg, 0.048 mmol). Yield: 16%.

^{1}H NMR (600 MHz, DMSO-d_6, 25 °C): δ = 1.37 (s, 6H; CH_3(py)), 1.57 (m, ^3J(H,H) = 6.9 Hz, 2H; $NCH_2CH_2CH_2NHCO$), 1.62 (br, 8H; $NCH_2CH_2CH_2NH$-(Sq)), 2.07 (s, 3H; CH_3N), 2.32 (br, 8H; CH_2N), 2.37 (br, 2H; CH_2N), 2.48 (s, 6H; CH_3(py)), 3.17 (q, ^3J(H,H) = 6.4 Hz, 2H; CH_2NHCO), 3.50 (br, 8H; CH_2NH(Sq)), 4.52 (s, 2H; CH_2OAr), 6.15 (s, 2H; CH(py)), 7.12 (d, ^3J(H,H) = 8.6 Hz, 2H, Ar), 7.28 (d, ^3J(H,H) = 8.6 Hz, 2H, Ar), 7.48 (br, 4H; NH(Sq)), 8.22 (br, 1H; NHCO);^{13}C NMR (75 MHz, DMSO-d_6, 25 °C) δ = 14.2, 21.7, 25.2, 33.5, 49.7, 52.7, 67.0, 79.2, 115.5, 121.3, 126.6, 129.2, 131.0, 142.0, 143.1, 154.8, 158.5, 167.5, 167.9, 182.4. HRMS (ESI) calcd for 892.4469 (M+Na; $C_{45}H_{58}BN_9O_6F_2Na^+$), found 892.4452.

Synthesis of Cyclosquaramide **2**. The free amine of **13** (400 mg, 0.68 mmol) was prepared as described for compound **1**. Then it was dissolved in DMSO (1.0 mL) and 2 equiv of diisopropylethylamine (240 μL, 1.38 mmol) was added to this solution and stirred for a few minutes. Fluorescein 5-isothiocyanate (FITC) (266 mg, 0.68 mmol) in DMSO (3 mL) was added to the solution and the reaction mixture was stirred at room temperature for 120 h under argon atmosphere and protected from direct light. The reaction mixture was filtered and purified by RP-HPLC (Column: XBridge Prep C18 OBD 5 μm, 19 × 150 mm, from Waters. Mobile phase: eluent A (H_2O, 10 mM $AcONH_4$, pH 9.0), eluent B (acetonitrile)) obtaining **2** as an orange solid (118 mg, 0.134 mmol). Yield: 20%.

^{1}H NMR (600 MHz, DMSO-d_6, 25 °C): δ = 1.67−1.72 (br, 10H; $CH_2CH_2CH_2$), 2.14 (br, 3H; NCH_3), 2.47−2.48 (br, 10H; NCH_2), 3.52 (br, 10H; CH_2NH(Sq)+CH_2NHCS), 6.54−6.65 (m, 7H; FITC), 7.17 (d, ^3J(H,H) = 8.2 Hz, 1H; FITC), 7.48 (br, 4H; NH), 7.72 (br, 1H; NH), 8.13, (br, 1H, SCNH), 8.22 (br, 1H, FITC), 9.95 (br, 1H, SCNH), 10.13 (br, 2H, OH); ^{13}C NMR (75 MHz, DMSO-d_6, 25 °C) δ = 221.7, 25.5, 27.7, 50.3, 53.6, 83.4, 102.4, 110.5, 113.7, 116.9, 118.4, 124.9, 128.9, 129.4, 136.7, 141.2, 152.7, 160.3, 167.9, 168.9, 172.9, 180.3, 182.2. HRMS (ESI) calcd for 879.3500 (M+H; $C_{45}H_{51}N_8O_9S^+$); found 879.3503.

Quantum Yield Determination. The fluorescence quantum yield for cyclosquaramides **1** (C2-BDP) and **2** (C2-FITC) were obtained in aqueous solutions H_2O−DMSO 1% at pH 7.4 (PBS, phosphate buffered saline) and pH 5.5 (cacodylate buffer, 0.05 M). Quantum yield of C2-BDP and C2-FITC was measured with Oregon Green 488 (OG) as standard (φ = 0.97; borate buffer 0.1 M pH 9) according to eq 1.

$$\varphi_u = \varphi_s \times \frac{I_u}{I_s} \times \frac{A_s}{A_u} \quad (1)$$

where ϕ is the quantum yield, I is the integrated emission intensity, A is the optical density (absorbance) at the excitation wavelength; u subscript refers to unknown quantum yield cyclosquaramides, and s subscript refers to standard fluorophore.

The integrated emission intensity, I, was calculated according to eq 2.

$$I = \sum_{i=WL_0}^{WL_f} [I_{WL}]_{WL_{i+1}} \cdot (WL_{i+1} - WL_i) \quad (2)$$

where WL_o is the initial acquisition wavelength of the emission spectra; WL_f is the final acquisition wavelength of the emission spectra and I_{WL} is the fluorescence intensity at a given wavelength. To obtain the quantum yield, sample solutions of C2-BDP and C2-FITC were prepared at three different concentrations in the required buffer. Solutions of the reference compound (OG) were prepared at three different concentrations in the standard conditions. All the concentrations used in this study were in the range of fluorescence linearity. At a given excitation wavelength, optical density and fluorescence emission spectra were recorded for unknown and standard solutions. Quantum yield was calculated by crossing unknown versus standard optical density and integrated fluorescence emission spectra values of the measured solutions as given in eq 1. The average of all values was obtained as the final quantum yield value.

Determination of the Binding Constants of Compound 4 with Phosphate Compounds by Isothermal Titration Calorimetry (ITC). ITC experiments were run to determine the unknown thermodynamic constants of adenosine 5′-monophosphate disodium salt (AMP), D-mannose 6-phosphate disodium salt hydrate (M6P), and D-fructose 1,6-bisphosphate trisodium salt hydrate (FBP). For this purpose, solutions of the phosphate compounds in distilled water were titrated against HCl solution in distilled water. For further details on host−guest concentrations used and the equilibria fitted to obtain the binding constant, see the Supporting Information.

The binding constants of 5 with the different phosphates were determined at 25 °C. Mixture solutions of compound 5 (host) and the respective phosphates (guest) in water were titrated against an HCl solution in distilled water. For further details on host−guest concentrations used and the equilibria fitted to obtain the binding constant, see the Supporting Information.

Evaluation of the pH Dependence of the Fluorescence Emission of Cyclosquaramides 1 (C2-BDP) and 2 (C2-FITC). Sixteen different 5 × 10^{-6} M solutions of cyclosquaramides **1** and **2** at pH varying from 3 to 11 were prepared in H_2O−DMSO 1%, with constant ionic strength (0.1 M NaCl).

The pH values of the water solutions were adjusted as follows. For acidic solutions, 1 mL of acetic acid was diluted in

dx.doi.org/10.1021/bc500258b | Bioconjugate Chem. 2014, 25, 1537−1546

20 mL of water with constant ionic strength (0.1 M NaCl). The pH of this solution was adjusted with 3 M HCl to decrease pH or NH_3 to increase it until the desired pH was reached. For alkaline solutions, the same procedure was applied starting with 1 mL of concentrated ammonia and using 1 M NaOH or acetic acid to adjust pH. 5×10^{-4} M solutions of compounds **1** and **2** were prepared in DMSO. Then, 40 μL of the DMSO solutions were added to 3.96 mL of each buffered solution and the final volume was adjusted to obtain 4 mL of 5×10^{-6} M solutions at the varying pH (3−11) for each compound. These samples were stored in darkness and thermostated at 37 °C for 5 min. After that, 3 fluorescence spectra were recorded for each sample at excitation wavelengths of 480 and 440 nm for **1** and **2**, respectively. Once the spectra were recorded, the pH value of each solution was measured with a Crison 52 08 pH electrode (3 mm). Final representation is given as the averaged integrated emission fluorescence spectra versus the measured pH value for each solution.

Cell Lines and Cell Culture. NIH3T3 (nontransformed mouse fibroblasts) were from ATCC, U87MG (human glioma cells) were kindly provided by Dr. Joan Seoane (Institut de Recerca Hospital Universitari Vall d'Hebron, Barcelona), and Jurkat cells (acute human T cell leukemia) were a gift from Prof. Joan Gil (IDIBELL, Barcelona). NIH3T3 and U87MG cells were maintained in DMEM (Dulbecco's Modified Eagle Medium (Sigma-Aldrich, St. Louis, MO, USA) medium. Jurkat cells were maintained in RPMI (Sigma-Aldrich, St. Louis, MO, USA). All media were supplemented with 10% inactivated fetal calf serum (Sigma Chemical Co., St. Louis, MO, USA) and penicillin−streptomycin (100 U/mL−100 mg/mL from Sigma-Aldrich, St Louis, MO, USA). All cell lines were grown under humidified air containing 5% CO_2 at 37. All cell lines were subconfluently grown and passaged, routinely tested for mycoplasma contamination and subjected to frequent morphological tests and growth curve analysis as quality control assessments. All cell lines were treated at a prophylactic concentration of 5 μg/mL with Plasmocin (Invivo Gen, San Diego, CA).

Cell Viability Analysis. Cultured cells viability was tested using CellTiter-Glo Luminescent Cell Viability Assay (Promega, Madison, WI). This is a homogeneous method to determine the number of viable cells in culture based on quantization of the ATP present as indicator of metabolically active cells. Cells lines were plated in a 96-well plate, 5000 cells/well in a final volume of 200 μL. Cells were treated with the appropriate amount (μL) of a 10 mM solution of fluorescent cyclosquaramide in PBS to reach a final 10 μM concentration in culture medium, and evaluated at different times from 8 to 48 h. After the treatment, cells were incubated with 25 μL of culture medium and 25 μL CellTiter-Glo reagent. Luminescence was measured using a Synergy Mx microplate reader (Biotek, Winooski, VT). All experiments were performed in triplicate.

Fluorescence Analysis by Flow Cytometry. Adherent cells lines (NIH3T3 and U87MG) were plated in 12-well plate, 100 000 cells/well; meanwhile, suspension cell line (Jurkat) was seeded in 24-well plate, 400 000 cells/well. Cells were treated with the appropriate amount (μL) of a 10 mM solution of fluorescent cyclosquaramide in PBS to reach a final 10 μM concentration in culture medium and incubated for a period of time varying depending on the experimentat at 37 °C. After the treatment, cells were trypsinized and centrifuged for 5 min at 1800 rpm, washed with PBS 1×, centrifuged for additional 5 min, and resuspended in Isoton buffer. Sample fluorescence was quantified by laser flow cytometry.

Fluorescence Analysis by Fluorescent Confocal Laser Scanning Microscopy. 40 000 cells/plate were plated in coverslips and treated with the appropriate amount (μL) of a 10 mM solution of fluorescent cyclosquaramide in PBS to reach a final 10 μM concentration in culture medium for 1 h at 37 °C unless otherwise stated. After the treatment, cell lines were washed twice with PBS 1× and fixed with 4% formaldehyde, and incubated for 20 min at room temperature. Later, cell line coverslips were washed twice with PBS 1× and permeabilized with PBS/Triton 0.2% for 20 min at room temperature. Finally, cells line coverslips were mounted with Fluorescent Mounting Medium (Dako, and Carpinteria, CA) and analyzed by fluorescent confocal laser scanning microscopy. Images were obtained at 2048 × 2048 pixels and captured at 63× objective. The excitation wavelengths used were 480 nm for C2-BDP and C2-FITC, and 405 nm for C2-PY.

C2-BDP Subcellular Localization Studies. Commercially available organelle stains were used as counterstains of Early Endosome, Late Endosome, and Lysosome and Golgi organelles. Selected CellLight stains are based in the BacMam system. This system consists in modified insect virus, expressing a fusion construct of an endocytic pathway protein linked with red fluorescent protein (RFP). NIH3T3 and U87MG cell line were plated on coverslips in 24 well-plates, 40 000 cells/well. Cells were incubated with 12 μL of each stain system to obtain 40 viral particles for 24 h at 37 °C. Then, cells were treated with C2-BDP to reach a final 10 μM concentration in culture media for 1 h at 37 °C. Carefully, to avoid cell detachment, cells were washed, fixed, stained with DAPI (nucleus), and mounted to obtain preparations suitable for fluorescent confocal laser scanning microscopy analysis. C2-BDP fluorescence was excited at 488 nm line of an Ar laser with emission recorded between 502 and 535, and Bacman-RFP proteins were excited with 532 nm He−Ne lasers with emission recorded between 594 and 635 nm. Images were 2048 × 2048 pixels and captured with 63× objective. Images obtained were merged using Adobe Photoshop CS3 (Adobe Systems, Mountain View, CA).

■ ASSOCIATED CONTENT

Ⓢ Supporting Information

Experimental procedures and methods including NMR spectra, binding studies, curve fitting, cell culture, and confocal microscopy images. This material is available free of charge via the Internet at http://pubs.acs.org.

■ AUTHOR INFORMATION

Corresponding Authors

*E-mail: (A.C.) antoni.costa@uib.es.
*E-mail: (C.R.) carmen.rotger@uib.es.

Notes

The authors declare no competing financial interest.

■ ACKNOWLEDGMENTS

This work was supported by the Ministry of Economy and Competitivity (grants CTQ2011-27152 and Consolider-Ingenio CSD2010-00065) and CAIB (grant 23/2011, FEDER funds).

REFERENCES

(1) Han, J., Loudet, A., Barhoumi, R., Burghardt, R. C., and Burgess, K. (2009) A ratiometric pH reporter for imaging protein-dye conjugates in living cells. *J. Am. Chem. Soc. 131*, 1642−1643.

(2) Doorley, G. W., and Payne, C. K. (2012) Nanoparticles act as protein carriers during cellular internalization. *Chem. Commun. 48*, 2961−2963.

(3) Guo, X., and Huang, L. (2012) Recent advances in nonviral vectors for gene delivery. *Acc. Chem. Res. 45*, 971−979.

(4) Cadossi, R., Ronchetti, M., and Cadossi, M. (2014) Locally enhanced chemotherapy by electroporation: clinical experiences and perspective of use of electrochemotherapy. *Future Oncol. 10*, 877−890.

(5) Zhang, Y., and Yu, L.-C. (2008) Microinjection as a tool of mechanical delivery. *Curr. Opin. Biotechnol. 19*, 506−510.

(6) Mishra, A., Lai, G. H., Schmidt, N. W., Sun, V. Z., Rodriguez, A. R., Tong, R., Tang, L., Cheng, J., Deming, T. J., Kamei, D. T., and Wong, G. C. L (2011) Translocation of HIV TAT peptide and analogues induced by multiplexed membrane and cytoskeletal interactions. *Proc. Natl. Acad. Sci. U.S.A. 108*, 16883−16888.

(7) Rothbard, J. B., Jessop, T. C., Lewis, R. S., Murray, B. A., and Wender, P. A. (2004) Role of membrane potential and hydrogen bonding in the mechanism of translocation of guanidinium-rich peptides into cells. *J. Am. Chem. Soc. 126*, 9506−9507.

(8) Schmidt, N., Mishra, A., Lai, G. H., and Wong, G. C. (2010) Arginine-rich cell-penetrating peptides. *FEBS Lett. 584*, 1806−1813.

(9) Villalonga, P., Fernandez de Mattos, S., Ramis, G., Obrador-Hevia, A., Sampedro, A., Rotger, C., and Costa, A. (2012) Cyclosquaramides as kinase inhibitors with anticancer activity. *ChemMedChem 7*, 1472−1480.

(10) Lee, C.-W., Cao, H., Ichiyama, K., and Rana, T. M. (2005) Design and synthesis of a novel peptidomimetic inhibitor of HIV-1 Tat−TAR interactions: Squaryldiamide as a new potential bioisostere of unsubstituted guanidine. *Bioorg. Med. Chem. Lett. 15*, 4243−4246.

(11) Kumar, S. P., Glória, P. M. C., Gonçalves, L. M., Gut, J., Rosenthal, P. J., Moreira, R., and Santos, M. M. M. (2012) Squaric acid: a valuable scaffold for developing antimalarials? *MedChemComm 3*, 489−493.

(12) Olmo, F., Rotger, C., Ramírez-Macías, I., Martínez, L., Marín, C., Carreras, L., Urbanová, K., Vega, M., Chaves-Lemaur, G., Sampedro, A., Rosales, M. J., Sánchez-Moreno, M., and Costa, A. (2014) Synthesis and biological evaluation of N,N′-squaramides with high in vivo efficacy and low toxicity: toward a low-cost drug against chagas disease. *J. Med. Chem. 57*, 987−999.

(13) Buurman, E. T., Foulk, M. A., Gao, N., Laganas, V. A., McKinney, D. C., Moustakas, D. T., Rose, J. A., Shapiro, A. B., and Fleming, P. R. (2012) Novel rapidly diversifiable antimicrobial RNA polymerase switch region inhibitors with confirmed mode of action in *Haemophilus influenza*. *J. Bacteriol. 194*, 5504.

(14) Janetka, J. W., and Ashwell, S. (2009) Checkpoint kinase inhibitors: a review of the patent literature. *Expert Opin. Ther. Pat. 19*, 165−197.

(15) Crew, A., Li, A. H., Qiu, L., Castelhano, A., Dong, H., Smith, A., Tardibono, L., and Zhang, T. (2006) (Arylamidoaryl)Squaramide compounds. (OSI Pharmaceuticals Inc.). Patent No WO/2006/034111.

(16) Quinonero, D., Prohens, R., Garau, C., Frontera, A., Ballester, O., Costa, A., and Deya, P. M. (2002) A therical study of aromaticity in squaramide complexes with anions. *Chem. Phys. Lett. 351*, 115−120.

(17) Soberats, B., Martinez, L., Sanna, E., Sampedro, A., Rotger, C., and Costa, A. (2012) Janus-like squaramide-based hosts: dual mode of binding and conformational transitions driven by ion-pair recognition. *Chem.—Eur. J. 18*, 7533−7542.

(18) López, C., Sanna, E., Carreras, L., Vega, M., Rotger, C., and Costa, A. (2013) Molecular recognition of zwitterions: enhanced binding and selective recognition of miltefosine by a squaramide-based host. *Chem. Asian. J. 8*, 84−87.

(19) Alemán, J., Parra, A., Jiang, H., and Jorgensen, K. A. (2011) Squaramides: bridging from molecular recognition to bifunctional organocatalysis. *Chem.—Eur. J. 17*, 6890−6899.

(20) Garau, C., Frontera, A., Ballester, P., Quiñonero, D., Costa, A., and Deya, P. M. (2005) A theoretical ab initio study of the capacity of several binding units for the molecular recognition of anions. *Eur. J. Org. Chem.*, 179−183.

(21) Rotger, C., Soberats, B., Quiñonero, B., Frontera, A., Ballester, P., Benet-Buchholz, J., Deyà, P. M., and Costa, A. (2008) Crystallographic and theoretical evidence of anion-pi and hydrogen-bonding interactions in a squaramide-nitrate salt. *Eur. J. Org. Chem.*, 1864−1868.

(22) Tungen, J. E., Nolsøe, J. M. J., and Hansen, T. V. (2012) Asymmetric iodolactonization utilizing chiral squaramides. *Org. Lett. 14*, 5884−5887.

(23) Prohens, R., Rotger, M. C., Piña, M. N., Deyà, P. M., Morey, J., Ballester, P., and Costa, A. (2001) Thermodynamic characterization of the squaramide-carboxylate interaction in squaramide receptors. *Tetrahedron Lett. 42*, 4933−4936.

(24) Piña, M. N., Rotger, C., Soberats, B., Ballester, P., Deyà, P. M., and Costa, A. (2007) Evidence of anion-induced dimerization of a squaramide-based host in protic solvents. *Chem. Commun.*, 963−965.

(25) Piña, M. N., Soberats, B., Rotger, C., Ballester, P., Deyà, P. M., and Costa, A. (2008) Selective sensing of competitive anions by non-selective host: The case of sulfate and phosphate in water. *New J. Chem. 32*, 1919−1923.

(26) Delgado-Pinar, E., Rotger, C., Costa, A., Piña, M. N., Jiménez, H. R., Alarcón, J., and García-España, E. (2012) Grafted squaramide monoamine nanoparticles as simple systems for sulfate recognition in pure water. *Chem. Commun. 48*, 2609−2611.

(27) Jin, C., Zhang, M., Wu, L., Guan, Y., Pan, Y., Jiang, J., Lin, C., and Wang, L. (2013) Squaramide-based tripodal receptors for selective recognition of sulfate anion. *Chem. Commun. 49*, 2025−2027.

(28) Li, J.-S., Wang, H., Cao, L.-W., and Zhang, H.-S. (2006) 8-Phenyl-(4-oxy-acetic acid N-hydroxysuccinimidyl ester)-4,4-difluoro-1,3,5,7-tetramethyl-4-bora-3a,4a-diaza-s-indacene as a new highly fluorescent-derivatizing reagent for aliphatic amines in disease-related samples with high-performance liquid chromatography. *Talanta 69*, 1190−1199.

(29) Rotger, C., Piña, M. N., Frontera, A., Martorell, G., Ballester, P., Deyà, P. M., and Costa, A. (2004) Conformational preferences and self-template macrocyclization of squaramide-based foldable modules. *J. Org. Chem. 69*, 2302−2308.

(30) Prohens, R., Martorell, G., Ballester, P., and Costa, A. (2001) A squaramide fluorescent ensemble for monitoring sulphate in water. *Chem. Commun.*, 1456−1457.

(31) Smith, S. A., and Pretorius, W. A. (2002) Spectrophotometric determination of pKa values for fluorescein using activity coefficient corrections. *Water SA 28*, 395−402.

(32) Boens, N., Leen, V., and Dehaen, W. (2012) Fluorescent indicators based on BODIPY. *Chem. Soc. Rev. 41*, 1130−1172.

(33) Loudet, A., and Burgess, K. (2007) BODIPY dyes and their derivatives: syntheses and spectroscopic properties. *Chem. Rev. 107*, 4891−4932.

(34) Kálai, T., and Hideg, K. (2006) Synthesis of new, BODIPY based sensors and labels. *Tetrahedron 62*, 10352−10360.

(35) The Pearson's correlation coefficient (*P*) and the Mander's overlap coefficients (*M*1 and *M*2) used to quantify the degree of colocalization between fluorophores were obtained using Colog Fiji's pluging software: Schindelin, J., Arganda-Carreras, L., Frise, E., Kaynig, V., Longair, M., Pietzsch, T., Preibisch, S., Rueden, C., Saalfeld, S., Schmid, B., Tinevez, J.-Y., White, D. J., Hartenstein, V., Eliceiri, K., Tomancak, P., and Cardona, A. (2012) Fiji: an open-source platform for biological-image analysis. *Nat. Methods 9*, 676−682.

(36) Casey, J. R., Grinstein, S., and Orlowsk, J. (2010) Sensors and regulators of intracellular pH. *Nat. Rev. Mol. Cell Biol. 11*, 50−61.

(37) Dinesh, N. V. S, Bhupathiraju, K., Graça, M., and Vicente, H. (2013) Synthesis and cellular studies of polyamine conjugates of a mercaptomethyl−carboranylporphyrin. *Bioorg. Med. Chem. 21*, 485−495.

(38) Soulet, D., Gagnon, B., Rivest, S., Audette, M., and Poulin, R. (2004) A fluorescent probe of polyamine transport accumulates into

intracellular acidic vesicles via a two-step mechanism. *J. Biol. Chem. 279*, 49355−49366.
(39) Competitive C2-BDP cell uptake studies using a cocktail of four different natural polyamines (spermine, spermidine, putrescine, and cadaverine) showed that the C2-BDP up take was not significantly decreased under these conditions. In these experiments U87 cells were treated with a 200 μM concentration of each polyamine for 30 min or1 h and then with 10 μM C2-BDP for 1 h. Cell fluorescence was measured by flowcytometry.
(40) Crowley, K. S., Phillion, D. P., Woodard, S. S., Schweitzer, B. A., Singh, M., Shabany, H., Burnette, B., Hippenmeyer, P., Heitmeier, M., and Bashkin, J. K. (2003) Controlling the intracellular localization of fluorescent polyamide analogues in cultured cells. *Bioorg. Med. Chem. Lett. 13*, 1565−1570.
(41) Fortuna, A., Alves, G., Soares-da-Silva, P., and Falcão, A. (2012) Optimization of a parallel artificial membrane permeability assay for the fast and simultaneous prediction of human intestinal absorption and plasma protein binding of drug candidates: application to dibenz[b,f]azepine-5-carboxamide derivatives. *J. Pharm. Sci. 101*, 530−540.
(42) Faller, B. (2008) Artificial membrane assays to assess permeability. *Curr. Drug Metab. 9*, 886−892.
(43) Xiang, S., Tong, H., Shi, Q., Fernandes, J. C., Jin, T., Dai, K., and Zhang, X. (2012) Uptake mechanisms of non-viral gene delivery. *J. Controlled Release 158*, 371−378.
(44) Doherty, G. J., and McMahon, H. T. (2009) Mechanisms of endocytosis. *Annu. Rev. Biochem. 78*, 857−902.
(45) Data were fitted to a model comprising specific and non-specific binding, and performed using *GraphPad Prism* v 5.0f for Mac OS X, GraphPad Software, La Jolla California USA, www.graphpad.com.
(46) Parry, M. J., Alakoskela, J-M. I., Khandelia, H., Kumar, S. A., Jäättelä, M., Mahalka, A. K., and Kinnunen, P. K. J. (2008) High-affinity small molecule-phospholipid complex formation: binding of siramesine to phosphatidic acid. *J. Am. Chem. Soc. 130*, 12953−12960.
(47) Ghosh, P., Dahms, M. N., and Kornfeld, S. (2003) Mannose 6-phosphate receptors: new twists in the tale. *Nat. Rev. Mol. Cell. Biol. 4*, 202−212.
(48) Müller-Loennies, S., Galliciotti, G., Kollmann, K., Glatzel, M., and Braulke, T. (2010) A novel single-chain antibody fragment for detection of mannose 6-phosphate-containing proteins: application in mucolipidosis type II patients and mice. *Am. J. Pathol. 177*, 240−247.